Plant Arbovirus Mobilizes a Vector Salivary Protein to Initiate Plant Infection

Authors' names

Jing Zhao[1, 3], Jie Yang[1, 3], Xiangyi Meng[1, 3], Rongxiang Fang[1, 2], Yan Huo[1, 2, *], Lili Zhang[1, 2, *]

Authors' affiliations

[1] State Key Laboratory of Plant Genomics, Institute of Microbiology, Chinese Academy of Sciences, Beijing 100101, China.

[2] CAS Center for Excellence in Biotic Interactions, University of Chinese Academy of Sciences, Beijing 100049, China

[3] University of the Chinese Academy of Sciences, Beijing 100049, China.

***Corresponding author**

* Address correspondence to: Dr. Lili Zhang, Institute of Microbiology, Chinese Academy of Sciences, No 3, Yard 1, West Beichen Road, Chaoyang, Beijing 100101, China. Phone (+86)10-64806915; Fax (+86)10-64806543; E-mail: Zhangll@im.ac.cn

* Address correspondence to: Dr. Yan Huo, Institute of Microbiology, Chinese Academy of Sciences, No 3, Yard 1, West Beichen Road, Chaoyang, Beijing 100101, China. Phone (+86)10-64806915; Fax (+86)10-64806543; E-mail: huoy@im.ac.cn

Abstract

Plant arboviruses rely heavily on insects' feeding activities for successful transmission. Insect salivary proteins have been suggested to be essential for successful viral infection, but their exact mechanisms are largely unknown. In this study, we reveal that salivary factors from *Laodelphax striatellus* are necessary for infection of *Rice stripe virus* (RSV) in plants. A salivary carbonic anhydrase (LssaCA) is identified as an essential factor in promoting RSV infection. LssaCA interacts with a rice thaumatin-like protein (OsTLP) that has endo-β-1,3-glucanase activity and can degrade callose in plants. RSV infection induces callose deposition, which can be reversed by LssaCA. Furthermore, LssaCA directly binds to the RSV nucleocapsid protein (NP) in salivary glands, and the LssaCA-RSV NP complex still binds OsTLP and further increases its glucanase activity. This study provides new insights into the tripartite virus-insect vector-plant interaction, which is relevant to many agriculturally important plant arboviruses whose transmission is facilitated by insect salivary proteins.

Keywords: *Rice stripe virus*, *Laodelphax striatellus*, viral horizontal transmission, watery saliva protein, carbonic anhydrase, callose deposit, rice thaumatin-like protein, β-1,3-glucanase

Introduction

During plant virus transmission by piercing-sucking insects, arboviruses are inoculated into the plant phloem *via* the secreted insect's saliva (Arca & Ribeiro, 2018; Conway et al., 2016; Wu, Yi, Lv, Mao, & Wei, 2022). Thus, insect saliva acts as an interface for the virus-insect-host tripartite interaction and it can directly promote pathogen transmission to, and infection of, the hosts (Sun et al., 2020; Wu et al., 2022). However, despite the importance of insect salivary proteins in the tripartite interaction, there is still much to learn about how these proteins enable successful viral infection.

Previous studies have revealed that there are two ways in which insect saliva facilitates viral infection (Arca & Ribeiro, 2018). One is an indirect approach whereby the saliva modulates the host microenvironment at the feeding site, and saliva effectors work together to allow the arthropod to go unnoticed while it feeds on the host plant (Acevedo et al., 2019; Arca & Ribeiro, 2018; Sun et al., 2020). The other is direct regulation, whereby saliva proteins promote virus transmission through specific molecular interactions (Wen et al., 2019). Our recent work indicated that a *Laodelphax striatellus* mucin protein, LssaMP, enables the formation of the salivary sheath and facilitates the transmission of *rice stripe virus* (RSV) into the rice phloem (Huo et al., 2022). A recent study on leafhoppers revealed that the expression of a saliva calcium-binding protein is inhibited by *rice gall dwarf virus* (RGDV), thus causing an increase of cytosolic Ca^{2+} levels in rice and triggering callose deposition and H_2O_2 production. This increases the frequency of insect probing, thereby enhancing viral horizontal transmission into the rice phloem (Wu et al., 2022). Direct saliva protein-pathogen interactions have been reported in animal pathogens. For example, during transmission of *Borrelia burgdorferi* by *Ixodes scapularis*, the saliva protein Salp15 of *I. scapularis* binds to the bacterial outer surface protein C, which prevents the bacterium from being recognized by the animal immune system. In this way, the saliva protein enables the pathogen to infect the animal host (Ramamoorthi et

al., 2005; Schuijt et al., 2008). The *Anopheles gambiae* saliva sporozoite-associated protein (AgSAP) binds to the surface of the *Plasmodium berghei* sporozoite. The binding of AgSAP to heparan sulfate inhibits local inflammatory responses, thereby facilitating early *Plasmodium* infection in the vertebrate host. Although most plant viruses are completely dependent on insect vectors for plant-to-plant transmission (Gray, 2008), the direct function of insect saliva proteins in mediating virus transmission remains largely uninvestigated.

During sap-feeding, arthropods produce two distinct types of saliva at different stages of the feeding process; gel saliva and watery saliva (Bonaventure, 2012; Lou et al., 2019). The former forms a salivary sheath to provide a smooth path for the stylet penetration (Lou et al., 2019). The latter is secreted into the phloem sieve elements to prevent them from plugging up, suppresses plant defense responses, induces pattern-triggered immunity (PTI) through herbivore-associated molecular patterns (HAMPs), and induces effector-triggered immunity (ETI) through avirulent gene, etc. (Huang, Liu, Xu, Bao, & Zhang, 2017; Ji et al., 2017; Yi, Wu, & Wei, 2021).

For phloem-feeding insects, callose deposited on phloem sieve tubes can function as a defense mechanism by reducing insect feeding and preventing long-distance viral movement (Hao et al., 2008; Hipper, Brault, Ziegler-Graff, & Revers, 2013; Will & Vilcinskas, 2015; Zavaliev, Ueki, Epel, & Citovsky, 2011). Callose is a β-(1,3)-D-glucan polysaccharide that is synthesized by callose synthases and degraded by β-(1,3)-glucanases. Plants can defend themselves by depositing callose at the sieve tubes in response to virus infection, whereas viruses can counter this by activating β-(1,3)-glucanases to degrade callose and unplug the sieve tube occlusions (Bucher et al., 2001; Hao et al., 2008; Wu et al., 2022; Zavaliev et al., 2011).

RSV is the causative agent of rice stripe disease, a serious disease of rice crops that has occurred repeatedly in China, Japan, and Korea (Xu, Fu, Tao, & Zhou, 2021). RSV is completely dependent on insect vectors for transmission to its host plants, and *L. striatellus* is the main vector (Xu et al., 2021; Zhao et al., 2018). *L. striatellus*

transmits RSV in a persistent-propagative manner. The virus initially infects the midgut, then disperses from the hemolymph into the salivary glands, and is inoculated into the plant host during *L. striatellus* feeding (Huo et al., 2022). *L. striatellus* belongs to the order Hemiptera, whose members mainly feed from sieve tubes through their mouthparts (stylets) that penetrate plant tissues and reach sieve tubes to ingest the phloem sap (Tjallingii, 2006; van Bel & Will, 2016). RSV is secreted into the rice phloem *via* the watery saliva (Huo et al., 2022; Wang & Blanc, 2021).

In this study, we identified a molecular interaction among RSV, an *L. striatellus* saliva protein, and a plant β-1,3-glucanase. The insect saliva protein directly binds to the RSV nucleocapsid protein (NP) and then binds to a rice thaumatin-like protein to activate its β-1,3-glucanase activity. The activation of β-1,3-glucanase helps facilitate RSV infection of the host plant by inhibiting callose deposition in response to viral infection.

Results

L. striatellus ***salivary carbonic anhydrase is an essential factor in enhancing RSV infection***

To investigate the influence of *L. striatellus* salivary proteins on RSV infection levels in rice plants, two experiments were conducted and compared: viruliferous insect feeding (VIF) and microinjection of purified virus (MPV) (Fig. 1A). The results showed that VIF caused high RSV infection levels and obvious rice stripe disease symptoms, while MPV did not lead to disease symptoms, and only a low level of RSV NP protein was detected inside the plant (Fig. 1B-E). These results suggested that the insect saliva factors are necessary for enabling RSV infection.

To identify the salivary proteins that play roles in mediating RSV infection, we have sequenced the *L. striatellus* saliva proteins and focused on the watery proteins that were inoculated into the plant phloem sieve tubes together with RSV (Huo et al., 2022). A salivary protein, Sap6 (GenBank accession No. RZF48846.1), was identified to have a high expression level in *L. striatellus* salivary glands (Fig. 2A). Western blotting assay showed that Sap6 was secreted into the plant as a watery saliva protein (Fig. 2B-C). Sequence homology analysis revealed Sap6 as a carbonic anhydrase-like protein, and enzyme active site analysis and enzyme activity experiment indicated Sap6 as a carbonic anhydrase (Fig. 2D-E). Sap6 was then named *L. striatellus* salivary carbonic anhydrase (LssaCA).

To determine the role of LssaCA in RSV infection of rice plants, a *LssaCA*-specific double-stranded RNA (dsLssaCA) was synthesized and delivered into the hemocoel of RSV-infected 3rd instar nymphs to interfere with the gene expression. At 2 days post-microinjection (dpi), the *LssaCA* mRNA levels were measured by RT-qPCR and compared with the dsGFP control. The results showed that dsLssaCA treatment reduced the *LssaCA* mRNA level by 80% (Fig. 3A). The two groups of insects were then allowed to feed on healthy rice seedlings (5 insects per

rice seedling) for 2 days. The RSV NP RNA levels (indicative of RSV titers) in the plants were measured at 14 days post-feeding (dpf). Compared with the rice seedlings fed by dsGFP-treated insects, those fed by dsLssaCA-treated insects had significantly reduced RSV titers (Fig. 3B), indicating that LssaCA played an essential role in mediating RSV infection of the rice plants.

LssaCA enhances RSV infection not before the viruses have been inoculated into the plant phloem

To determine at which step LssaCA-deficiency affected RSV infection, we analyzed the influence of LssaCA-deficiency on RSV titers during several steps of the RSV transmission process, including the virus load in the salivary glands and saliva, and the initial inoculation levels *in planta*. First, at 2 days after dsLssaCA treatment of the viruliferous insects when *LssaCA* was significantly downregulated, RT-qPCR was used to detect RSV titer in the insect salivary glands and the results showed that *LssaCA* deficiency did not reduce RSV titers in this tissue (Fig. 3C). Then, the LssaCA-deficient insects were allowed to feed on an artificial diet and their saliva was collected for RSV level analysis, which revealed that LssaCA-deficiency did not reduce the RSV titer in the secreted saliva (Fig. 3D). Finally, plants were fed with 10 viruliferous insects for 24 h respectively and the RSV titers were measured immediately after feeding, which showed that LssaCA-deficiency did not affect the RSV initial inoculation levels *in planta* (Fig. 3E). These results suggested that LssaCA promoted RSV infection by a mechanism occurred not in insects or early stage of viral entry in plants, but *in planta* after viral inoculation.

As shown in Fig. 1, VIF but not MPV is able to enable RSV infection of rice plants, suggesting the necessity of insect saliva factors in enabling RSV infection. To further confirm whether LssaCA played a role in directly enhancing RSV levels *in planta*, we produced a recombinant LssaCA protein to pre-incubate with purified RSV particle solution and used bovine serum albumin (BSA) as a control for comparison. The two groups were then microinjected into leaves on different plants, and at 14 dpi

their viral titers were measured using NP gene-specific RT-qPCR. The results showed that compared to those inoculated with BSA plus RSVs particles, those inoculated with LssaCA plus these same particles exhibited significantly higher RSV titer values (Fig. 3F-G). These findings clearly indicate that LssaCA plays an important role in promoting RSV infection of plants after RSV has been inoculated into the plant.

LssaCA interacts with rice thaumatin-like protein to increase its endo-β-1,3-glucanase activity

Because LssaCA played its role *in planta*, we performed two experiments to investigate the mechanisms by which LssaCA enhances RSV infection. The first was to create LssaCA mutant proteins lacking enzymatic activity to determine if the enhanced infection was related to the LssaCA enzymatic activity. The second was to conduct a yeast two-hybrid screening to identify rice proteins that interact with LssaCA.

LssaCA has 7 residues constituting the enzymatic active center, including H_{111}, N_{139}, H_{141}, H_{143}, E_{153}, H_{166}, and T_{253}. Seven recombinant mutant proteins were constructed and were labeled as LssaCA^{H111D}, LssaCA^{N139H}, LssaCA^{H141D}, LssaCA^{H143D}, LssaCA^{E153H}, LssaCA^{H166D}, LssaCA^{T253E} (Fig. S2A). Enzymatic activity assays indicated that five of the seven mutants had significantly reduced enzymatic activity (Fig. S2B). To measure the influence of these mutants on RSV infection, they were pre-cultured with purified RSV particle solution and were then microinjected into plant leaves. The RSV titers were measured using RT-qPCR at 14 dpi. The results showed that, compared to LssaCA, none of the mutants decreased the protein function in enhancing RSV infection (Fig. S2C). These results suggest that LssaCA enables RSV infection in an enzymatic activity-independent manner.

The yeast two-hybrid screening identified a rice thaumatin-like protein (XP_025879846.1), designated as *Oryza sativa* thaumatin-like protein (OsTLP) (Fig. 4A-B and S3). The open reading frame of OsTLP encoded for a polypeptide of 327 amino acids and a thaumatin family (THM) domain from residues 27 to 267. A

190 BLAST algorithm-based analysis against sequence databases revealed the sequence
191 identities to TLP 1b. The N-terminal 24 amino acids constituted a secretion signal
192 peptide, suggesting OsTLP as a secreted protein. Pull-down and MST assays were
193 performed to confirm the molecular interaction between OsTLP and LssaCA. The
194 pull-down assays showed that OsTLP and LssaCA had a specific interaction (Fig. 4C).
195 The MST assay revealed a K_D of 1.3 ± 2.2 μM for the OsTLP-LssaCA interaction,
196 further confirming the molecular interaction (Fig. 4D).

197 Previous studies have reported that TLP orthologs in apples, cherries, tomatoes,
198 barley, etc. have endo-β-1,3-glucanase activity, which works on degrading callose (de
199 Jesus-Pires et al., 2020). To confirm the endo-β-1,3-glucanase activity of OsTLP, an
200 enzyme activity experiment was conducted with the recombinantly expressed OsTLP
201 protein. The results revealed an average endo-β-1,3-glucanase activity of 60 units/mg
202 OsTLP (Fig. 4E). To determine the *in-planta* activity of OsTLP, OsTLP
203 overexpression transgenic plants were constructed. Enzymatic activity assays
204 confirmed that the transgenic plants had significantly increased β-1,3-glucanase
205 activity (Fig. 4F).

206 To investigate the influence of the molecular interaction between LssaCA and
207 OsTLP on OsTLP activity, OsTLP was pre-incubated with either LssaCA or a BSA
208 control for 2 h before the enzymatic activity was measured. The results showed that
209 pre-incubation with LssaCA significantly increased OsTLP activity, compared to the
210 BSA control (Fig. 4G). These results imply that LssaCA may facilitate RSV infection
211 by enhancing the activity of OsTLP to degrade callose.

212 ***LssaCA inhibits callose deposition induced by RSV infection***

213 Callose deposition on sieve plates is an important mechanism for slowing virus
214 long-distance transmission and reducing the virus infection level in plants (Li et al.,
215 2012; Zavaliev et al., 2011). To investigate whether RSV infection induces callose
216 deposition, rice seedlings were fed by RSV-free or viruliferous *L. striatellus* for 24 h,
217 and then callose deposition of the plants was measured. The results showed that VIF

218 led to more callose deposition compared with that induced by feeding with RSV-free
219 *L. striatellus* (Fig. 5A-B). ELISA assays also revealed an increased callose
220 concentration in the plant fed by viruliferous *L. striatellus* (Fig. 5C). To further
221 confirm the role of RSV in inducing callose deposition, the transcript levels of callose
222 synthase genes were measured using RT-qPCR. We found that RSV infection
223 upregulated *gsl3, gsl4, gsl5,* and *gsl10* (Fig. 5D–G). These results demonstrate that
224 RSV infection induces callose deposition.

225 To determine if LssaCA influences callose deposition induced by RSV infection,
226 we downregulated *LssaCA* in viruliferous *L. striatellus* by dsRNA microinjection. On
227 2 dpi when *LssaCA* expression was significantly reduced, the insects were allowed to
228 feed on healthy plants for 24 h, and then the callose deposition was measured. The
229 results showed that the plants fed by *LssaCA*-deficient insects deposited more callose
230 compared to the plants fed by the control-group insects (dsGFP treatment) (Fig. 5H–J),
231 indicating that LssaCA can impair the callose caused by RSV infection.

232 ***OsTLP degrades callose to facilitate RSV infection***

233 To confirm if OsTLP degrades the RSV-induced callose *in planta*, viruliferous *L.*
234 *striatellus* were allowed to feed on either *OsTLP* overexpression plants or control
235 plants, and then callose deposition was measured. The results showed that transgenic
236 plants exhibited significantly lower callose deposition compared to wild-type ones
237 (Fig. 6A-B), indicating that OsTLP can degrade the deposit callose induced by RSV
238 infection. Moreover, we measured the RSV infection levels that were influenced by
239 OsTLP overexpression. Viruliferous *L. striatellus* fed on either *OsTLP* overexpression
240 plants or control plants for 2 days, and then the RSV titers were measured on 14 dpf.
241 The RT-qPCR analyses indicated that, compared with wild-type plants, plants
242 overexpressing *OsTLP* had significantly higher RSV titers (Fig. 6C), indicating that
243 OsTLP facilitates RSV infection *in planta*. It is hypothesized that the overexpressed
244 OsTLP degrades the deposited callose that is caused by RSV infection, therefore
245 facilitating RSV infection.

246 ***RSV NP interacts with LssaCA to further enhance OsTLP enzymatic activity***

247 We have confirmed that LssaCA binds to OsTLP to promote callose degradation
248 and facilitates RSV infection *in planta*, we then investigated whether there is a direct
249 interaction between LssaCA and RSV by which RSV directly participates in the
250 function played by LssaCA. By using RSV and LssaCA-specific antibodies to
251 conduct immunofluorescence assays (IFA), we found that LssaCA and RSV
252 co-localized in salivary glands (Fig. 7A), suggesting a potential molecular interaction
253 between them. A pull-down assay then revealed a specific interaction between
254 LssaCA and RSV NP (Fig. 7B). An MST assay determined that the K_D of the
255 interaction between LssaCA and NP was 2.7 ± 2.2 μM, further confirming the
256 molecular interaction (Fig. 7C).

257 As LssaCA interacts with both RSV NP and OsTLP, we measured the tripartite
258 interaction. Through pull-down assays, we discovered that when LssaCA was
259 pre-incubated with RSV to form an NP-LssaCA complex, the complex still had the
260 ability to bind to OsTLP (Fig 7D). This result demonstrates a tripartite interaction
261 among these three proteins.

262 We then explored how the tripartite interaction affects OsTLP enzymatic activity.
263 OsTLP was pre-incubated with LssaCA-NP complex or LssaCA control. After
264 incubation for 2 h, the enzyme activity was measured. The results showed that
265 pre-incubation with LssaCA-NP complex significantly increased OsTLP activity
266 compared with LssaCA control (Fig. 7E), indicating that stronger activation of
267 β-1,3-glucanase activity was achieved through the NP-LssaCA-OsTLP tripartite
268 interaction.

269 Taken together, these results suggested that when RSV is delivered into plant
270 phloem, it can induce callose deposition. This process is overturned through a
271 tripartite interaction involving the LssaCA protein which binds to RSV in insect
272 salivary glands and then the LssaCA-RSV complex binds to OsTLP in plants. Once
273 this tripartite interaction occurs, OsTLP activity of β-1,3-glucanase is significantly

274 increased which degrades callose thus allowing for efficient RSV infection.

275

Discussion

Insects are known to be vectors of many plant viruses, and some of these plant viruses rely entirely on insect vectors for their plant-to-plant transmission. Previous studies have suggested that insect salivary proteins may facilitate arbovirus infection of plants through various mechanisms, such as breaking down plant cell walls, inhibiting plant immune defenses and callose deposition, directly binding to arbovirus to prevent their detection by plant immune systems, and more. Further research is needed to fully understand the role that insect salivary proteins play in arboviruses infection of plants. In this study, we have found that RSV infection of rice plants triggers the deposition of callose. However, this process is reversed by a tripartite interaction involving the central component of an insect salivary protein LssaCA, which subsequently binds to RSV in insect salivary glands and then OsTLP in the plants. The activity of OsTLP's β-1,3-glucanase is significantly increased when this tripartite interaction occurs; leading to the degradation of callose and thus allowing for efficient RSV infection (Fig. 8).

Callose is a complex polysaccharide, and its deposition in plant phloem plays an important role in defending against insect attacks and viral spread (Zavaliev et al., 2011). When attacked by piercing insects or viruses, plants activate callose deposition on the sieve plates to occlude the flow of phloem sap, thus discouraging feeding and reducing viral long-distance spread. This accumulation of callose in plant phloem can be switched on or off through the action of callose synthases and hydrolases (Li et al., 2012; Shangguan et al., 2018). Studies have shown that expression levels of these glucanase enzymes differ between resistant and susceptible plant species. This suggests that some plants may be more successful at resisting infection due to high levels of glucanase enzymes in their tissues, which allow them to more quickly and effectively form callose barriers against insects and viruses (Hao et al., 2008). Some insects have evolved β-1,3-glucanases enzymes that can degrade the deposited callose, thus enabling them to bypass the plant's defense mechanisms and continue feeding

304 (Bucher et al., 2001; Hao et al., 2008). In this study, we demonstrate a novel
305 mechanism by which an insect saliva protein binds to a plant β-1,3-glucanases protein,
306 thus activating the enzymatic activity and promoting callose degradation.

307 In this study, we found that plants fed on by viruliferous insects showed higher
308 callose deposition than did plants fed on by uninfected insects (Fig. 5A–C),
309 suggesting that arbovirus infection *via* insect saliva may represent a double stress to
310 the plant, inducing stronger callose deposition that must be overcome for successful
311 insect feeding and viral spread. To analyze how this happens, we looked at the
312 tripartite interaction between LssaCA-NP-OsTLP. We found that this interaction
313 induced significantly higher β-1,3-glucanase activity than the LssaCA-OsTLP
314 interaction alone, suggesting that SBPH and RSV have evolved mechanisms to
315 increase β-1,3-glucanase activity in order to bypass the plant's defense of callose
316 deposition and facilitate successful viral spread.

317 LssaCA is carbonic anhydrase, but its role in aiding RSV infection does not rely
318 on its enzymatic activity (Fig. S2). Our results found that even though LssaCA
319 mutants had significantly reduced enzymatic activity, their ability to facilitate RSV
320 infection was not significantly decreased. Because LssaCA interacts with RSV NP, we
321 measured the interactions between LssaCA mutants and NP. Pull-down assays
322 indicated that all the mutants still interacted with RSV NP (Fig. S4), while the mutants
323 with a stronger interaction (LssaCA^{H111D} and LssaCA^{E153H}) showed better facilitation
324 for RSV infection levels (Fig. S2). These results further supported the importance of
325 LssaCA-NP interaction in mediating RSV infection, while the exact role of LssaCA
326 enzymatic activities in aiding RSV infection is still unclear.

327 In conclusion, this study elucidated a tripartite interaction among a plant virus, an
328 insect saliva protein, and a host phloem β-1,3-glucanase. This interaction inhibited the
329 plant defense of callose deposition and enabled arboviral phloem transmission. This
330 study provides new insights into the tripartite virus-insect vector-plant interaction,
331 which is relevant to many agriculturally important plant arboviruses whose

transmission is facilitated *via* insect saliva proteins.

Figure 1. *Laodelphax striatellus* feeding is necessary for *Rice stripe virus* (RSV)to infect rice.

A. The schematic diagram shows the two methods of rice inoculation with RSV: viruliferous insect feeding (VIF) and microinjection of purified virus (MPV). Three-leaf rice seedlings were used and viral infection was detected three weeks after inoculation.

B-D. Plant symptoms of rice stripe disease were observed in the VIF group (B-D), including heart leaf curling (C) and the striped spots on the leaves (D), but not in the MPV group (B and D). C shows an enlarged image of the VIF-group leaves.

E. Western blots to show the levels of RSV infection in plants inoculated with VIF or MPV. Anti-RSV antibodies were used to detect the RSV titers in the plants.

Figure 2. Characteristics of the *L. striatellus* saliva carbonic anhydrase (LssaCA).

A. RT-qPCR analyses of *LssaCA* transcript levels in different tissues. R-body, the remaining body after removal of the guts, salivary glands, fat bodies, and ovaries.
B. Western blots showing LssaCA protein distribution in *L. striatellus* salivary glands (SBPH SG) and rice plants (Rice). The weaker signal in dsLssaCA-treated SBPH indicates a specific knockdown of LssaCA by dsLssaCA. Rice plants fed by SBPH acquire LssaCA (+SBPH), whereas control plants do not contain LssaCA protein (-SBPH).
C. Western blots showing the distribution of LssaCA in watery and gel saliva. Total watery or gel saliva proteins were detected by silver staining.
D. Schematic diagram of LssaCA protein sequence. SP, signal peptide; Carb_anhydrase domain, conserved eukaryotic-type carbonic anhydrase sequence. Triangles indicate seven predicted catalytically active residues.
E. Esterase activity of recombinantly expressed LssaCA protein.

359 **Figure 3. The influence of LssaCA deficiency on RSV transmission and viral**
360 **infection of plants.**

361 A. The efficiency of gene silencing as determined by RT-qPCR. Each dot represents
362 salivary glands from five RSV-infected third-instar nymphs.
363 B. RSV infection level in rice plants as determined by RT-qPCR. RSV infection
364 levels are represented by the copy number of the *NP* gene. Each dot represents
365 one rice plant fed on for 2 d and then grown for another 14 d.
366 C. RSV titers in *L. striatellus* salivary glands as determined by RT-qPCR. Each dot
367 represents salivary glands from five RSV-infected third-instar nymphs.
368 D. RSV titers in *L. striatellus* saliva as determined by RT-qPCR. Each dot represents
369 one saliva sample from 10 insects fed with an artificial diet.
370 E. RSV titers in rice plants as determined by RT-qPCR. Rice plants were fed for 24 h
371 and RSV titers were assayed immediately post-feeding. Each dot represents one
372 rice plant.
373 F. Schematic diagram to show the process of microinjecting an RSV particle
374 solution into a plant. The RSV was pre-incubated with BSA or recombinantly
375 expressed LssaCA protein before being microinjected into the plant phloem.
376 G. RT-qPCR to determine the level of RSV infection in microinjection-inoculated
377 rice. The titers of RSV (copy number of *NP*) in rice plants were measured at 14
378 days post-inoculation (dpi). BSA was used as a negative control. *, $p < 0.05$.

379 DsLssaCA and dsGFP indicate *LssaCA*- and *GFP*-specific dsRNA, respectively. ****,
380 $p < 0.0001$; **, $p < 0.01$; ns, not significant.

381 **Figure 4. The interaction between OsTLP and LssaCA plays a role in regulating**
382 **the enzymatic activity of OsTLP.**

383 A. Schematic diagram of the OsTLP protein sequence. SP, signal peptide; THM,
384 conserved thaumatin family protein sequence. Glyco_hydro_64 domain, glycoside
385 hydrolases of family 64.

386 B. Yeast two-hybrid assay showing the interaction between OsTLP and LssaCA. SD,
387 synthetically defined medium; Leu, Leucine; Trp, Tryptophan; His, Histidine;
388 3'AT, 3-amino-1,2,4-triazole; AD, transcription activation domain; BD,
389 DNA-binding domain.
390 C. Pull-down assays showing the interactions between LssaCA (LssaCA-His) and
391 OsTLP (MBP-OsTLP). MBP was used as a negative control. Both anti-His and
392 anti-MBP antibodies were used to detect corresponding proteins.
393 D. MST assay showing the interaction between LssaCA (LssaCA-His) and OsTLP
394 (MBP-OsTLP). MBP was used as a negative control. Bars represent SE.
395 E. The endo-β-1,3-glucanase activity of the purified recombinant OsTLP protein
396 (expressed as MBP-fusion protein). MBP was used to normalize results.
397 F. The endo-β-1,3-glucanase activity of OsTLP, which was overexpressed in
398 transgenic plants (OsTLP OE) or wild-type plants (WT).
399 G. Regulation of OsTLP enzymatic activity by LssaCA. ****, $p < 0.0001$.

400 **Figure 5. LssaCA inhibits RSV-induced callose deposition.**

401 A. Bright blue fluorescence of cross-sections showing callose deposition at feeding
402 sites. Samples were prepared from the leaf phloem of plants fed on by RSV-free
403 or RSV-infected *L. striatellus*. Thin sections were stained with 0.1% aniline blue
404 at 24 h after *L. striatellus* feeding and examined under a fluorescence microscope.
405 Xy, xylem; ph, phloem. Scale bars: 20 μm.
406 B. Average fluorescence intensity of arbitrary area of callose deposition counted
407 using ImageJ. Eight to ten random sites per sample were selected for the
408 evaluation of fluorescence intensity. ****, $p < 0.0001$.
409 C. Callose concentration in leaves of rice plants fed on by RSV-free or
410 RSV-infected *L. striatellus*. ****, $p < 0.0001$.
411 D–G. Transcript levels of callose synthase genes as determined by RT-qPCR. Insects
412 were allowed to feed on rice plants for 24 h before total RNAs were extracted. *,
413 $p < 0.05$; **, $p < 0.01$.

H. Bright blue fluorescence of cross-sections showing callose deposition at feeding sites. Samples were prepared from leaf phloem of plants fed on by dsGFP- or dsLssaCA-treated RSV-infected *L. striatellus*. Thin sections were stained with 0.1% aniline blue at 24 h after *L. striatellus* feeding and examined under a fluorescence microscope. Xy, xylem; ph, phloem. Scale bars: 20 μm.

I. Average fluorescence intensity of arbitrary area of callose deposition counted using ImageJ under a fluorescence microscope. Eight to ten random sites per sample were selected for the evaluation of fluorescence intensity. **, $p < 0.01$.

J. Callose concentration in leaves of rice plants fed on by dsGFP- or dsLssaCA-treated *L. striatellus*. **, $p < 0.01$.

Figure 6. OsTLP inhibits callose deposition to facilitate RSV infection.

A. Bright blue fluorescence of cross-sections showing callose deposition at feeding sites. Samples were prepared from the leaf phloem of plants fed on by RSV-infected *L. striatellus*. Scale bars: 20 μm. OsTLP OE, transgenic plants over-expressing OsTLP.

B. Average fluorescence intensity of arbitrary area of callose deposition counted using ImageJ under a fluorescence microscope. *, $p < 0.05$.

C. Promotion of RSV infection by OsTLP overexpression, as determined by RT-qPCR. Titers of RSV (copy number of *NP*) were measured at 14 days post-feeding. *, $p < 0.05$.

Figure 7. LssaCA-RSV NP interaction enhances the OsTLP enzymatic activity.

A. Immunofluorescence assay showing co-localization of RSV (shown in red) and LssaCA (shown in green) in *L. striatellus* salivary glands. Images are representative of three independent experiments with a total of 30 SBPHs analyzed. The scale bar represents 20 μm. psg, principal salivary gland; asg, accessory salivary gland.

440 B. GST pull-down assays show the interaction between LssaCA (GST-LssaCA) and
441 RSV NP (NP-His). GST was used as a negative control. Anti-GST and anti-His
442 antibodies were used to detect the corresponding proteins.
443 C. MST assay showing the interaction between LssaCA (LssaCA-His) and RSV NP
444 (GST-NP). GST was used as a negative control. Bars represent SE.
445 D. Pull-down assays showing the interaction between OsTLP (MBP-OsTLP) and
446 LssaCA-NP complex. LssaCA was expressed with a His tag and RSV NP was
447 expressed as a GST-fusion protein. LssaCA and NP were preincubated before
448 co-incubation with OsTLP. Anti-His and anti-GST antibodies were used to detect
449 the corresponding proteins.
450 E. Regulation of OsTLP enzymatic activity by LssaCA and LssaCA-NP. (LssaCA +
451 NP) indicates that the two proteins were pre-incubated before incubation with
452 OsTLP. ****, $p < 0.0001$.

453 **Figure 8. Proposed model of how RSV NP-LssaCA-OsTLP tripartite interaction**
454 **leads to callose degradation to promote RSV infection of plants.**

455 *L. striatellus* feeding on rice plants inoculates both RSV and LssaCA into the
456 phloem sieve elements. Within the plants, RSV induces callose synthesis, causing
457 callose deposition to inhibit RSV infection. However, LssaCA reverses this inhibition
458 by binding to OsTLP to enhance its β-1,3-glucanase activity, which degrades the
459 deposited callose. The interaction between RSV and LssaCA further enhances the
460 OsTLP enzymatic activity and facilitates RSV infection.

461 **Figure S1. Nucleotide sequence and deduced amino acid sequence of LssaCA.**

462 Underlining indicates the predicted signal peptide sequence. Seven predicted
463 catalytically active residues are shown in red. Bold font indicates eukaryotic-type
464 carbonic anhydrase sequences.

465 **Figure S2. LssaCA enzymatic activity does not affect RSV infection.**

466 A. Summary of the predicted enzymatic active sites and the muteins.

467 B. Relative esterase activities of recombinant LssaCA protein and its muteins. *, $p <$
468 0.05; **, $p < 0.01$; ****, $p < 0.0001$.

469 C. Schematic diagram to show the process of microinjecting RSV into a plant. The
470 RSV was pre-incubated with recombinantly expressed LssaCA, the LssaCA
471 muteins, or a BSA control, before being microinjected into the rice phloem.

472 D. The effects of LssaCA, its muteins, or the BSA control, on the levels of RSV
473 infection as determined by RT-PCR. The titers of RSV (copy number of *NP*)
474 were measured at 14 dpi.

475 **Figure S3. Nucleotide sequence and deduced amino acid sequence of OsTLP.**

476 Underlining indicates the predicted signal peptide sequence. Bold font indicates the
477 conserved thaumatin family protein sequence.

478 **Figure S4. The molecular interaction between RSV and LssaCA muteins is**
479 **important for RSV to infect rice plants.**

480 A. Pull-down assays showing the interactions between the LssaCA muteins
481 (expressed with a His-tag) and RSV NP (GST-NP). GST was used as a negative
482 control. Anti-His and Anti-GST represent antibodies against 6*His and GST,
483 respectively. Both $LssaCA^{H111D}$ and $LssaCA^{E153H}$ (marked in red) have a stronger
484 interaction with NP compared to the wild-type LssaCA protein.

485 B. Preincubation of RSV with either $LssaCA^{H111D}$ or $LssaCA^{E153H}$ facilitates RSV
486 infection of plants after being delivered via microinjection into the phloem. The
487 titers of RSV (copy number of *NP*) were measured at 14 dpi. BSA was used as a
488 negative control. *, $p < 0.05$; **, $p < 0.01$.

489 **Table S1. Primers used in this study.**

490

491 ## Materials and methods

492 ***Viruses, insects, host plants, and antibodies***

493 The RSV-free and RSV-infected *L. striatellus* individuals used in this study
494 were originally captured in Jiangsu Province, China, and were maintained in our
495 laboratory. All plants used to rear *L. striatellus* were grown in a growth incubator
496 (14.5 cm height, 3.2 cm radius) at 25°C under a 16-h light/8-h dark photoperiod.
497 Insects were transferred to fresh seedlings every 15 days to ensure adequate nutrition
498 and insect activity.

499 The RSV-specific antibody was produced using RSV ribonucleoproteins (RNPs)
500 as antigens. The LssaCA polyclonal antibody was produced using recombinantly
501 expressed LssaCA protein (with a His-tag at the C-terminus) as the antigen.

502 ***Tissue collection***

503 Insect dissection and tissue collection were performed using previously
504 described procedures (Huo et al., 2018). In brief, insects were anesthetized at 4°C for
505 10 min, and the forelegs were severed at the coxa-trochanter joint using forceps. The
506 hemolymph was expelled and drawn to the tip of clean forceps. The insects were then
507 dissected from the abdomen in pre-chilled PBS buffer. The fat body was collected
508 with forceps, aided by the tension of the liquid. Tissues, including the guts, salivary
509 glands, and ovaries, were washed three times in PBS to remove contaminants from
510 the hemolymph.

511 ***Bioinformatic analysis***

512 The signal peptide and transmembrane helix were predicted using tools at the
513 SignalP 5.0 server (https://services.healthtech.dtu.dk/service.php?SignalP-5.0) and the
514 TMHMM-2.0 server (https://services.healthtech.dtu.dk/service.php?TMHMM-2.0).
515 Homology searches of the protein sequence of LssaCA and OsTLP were conducted
516 using the BLAST algorithm at the National Center for Biotechnology Information
517 (http://blast.ncbi.nlm.nih.gov/Blast.cgi). Conserved domains were predicted with
518 SMART (http://smart.embl-heidelberg.de/).

519 ***Collection of watery and gel saliva***

520 Saliva was collected as described previously (Huo et al., 2022). Watery saliva
521 was obtained by centrifuging the collected artificial diet at 10,000 ×g for 10 min to
522 remove the solid gel. To collect gel saliva proteins, the membrane was washed twice
523 with PBS. Sheathes adhering to the parafilm were denatured and solubilized in a
524 solution consisting of 8 M urea, 4% v/v CHAPS, 0.1% w/v sodium dodecyl sulfate
525 (SDS), and 2% v/v DTT. The parafilm was incubated on an orbital shaker at room
526 temperature for 45 min. Then, the denatured gel saliva was concentrated to a final
527 volume of 100 μL. Saliva samples were collected from 2,000 insects for silver
528 staining and western blotting analyses.

529 ***Measurement of carbonic anhydrase activity***

530 Carbonic anhydrase activity was characterized by measuring its esterase activity.
531 *P*-nitroethyl acetate (*p*-NPA) was used as the substrate. The LssaCA enzyme solution
532 was prepared as follows: LssaCA was expressed in *E. coli* with a His-tag at the
533 C-terminus and the purified LssaCA protein was diluted in PBS buffer (pH 7.0) to a
534 final concentration of 1 mg/mL. Details of the reaction conditions have been
535 described elsewhere (Verpoorte et al., 1967). Briefly, 1 mL of freshly prepared 3 mM
536 *p*-NPA dissolved in acetone was added to 1.9 mL 100 mM PBS (pH 7.0), followed by
537 the addition of 0.1 ml LssaCA enzyme solution (0.5 mg/mL in 100 mM PBS). As the
538 blank control, 2 mL 100 mM PBS (pH 7.0) was added to 1 mL 3 mM *p*-NPA. The
539 absorbance at 384 nm was measured at the start of the reaction and 3 min later. One
540 unit (U) of enzyme activity is defined as the amount of enzyme that hydrolyzes 1
541 μmol *p*-nitroethyl acetate per minute at pH 7.0 at 25 °C.

542 ***Immunofluorescence assays***

543 Immunofluorescence assays (IFA) were performed to determine the localization
544 of RSV and LssaCA in *L. striatellus* salivary glands. The dissected salivary gland
545 samples were fixed in 4% v/v paraformaldehyde at 4°C overnight and then

546 permeabilized in 2% v/v Triton X-100 for 2 h. The samples were incubated with
547 rabbit anti-RSV serum and mouse anti-LssaCA serum (1:250 dilution in PBST/FBS:
548 PBS containing 2% v/v Triton X-100 and 2% fetal bovine serum) for 1 h at room
549 temperature. After washing twice with PBST, the samples were incubated with 1:200
550 diluted Alexa Fluor 488-conjugated goat anti-mouse antibody and Alexa Fluor
551 594-conjugated goat anti-rabbit antibody (Invitrogen) for 1 h. After washing three
552 times with PBST, the samples were examined under a Leica TCS SP8 microscope
553 (Leica, Wetzlar, Germany).

554 ***Evaluation of callose deposition in rice plants***

555 Five insects were allowed to feed on a 10 d-old rice plant in a leaf area of 2 × 2
556 cm for 24 h. The leaf samples were immersed in 5 mL alcoholic lactophenol (1
557 volume phenol: glycerol: lactic acid: water (1:1:1:1) and 2 volumes ethanol), then
558 evacuated with a syringe for 15 min, and then incubated at 65℃ for 30 min until the
559 chlorophyll was completely cleared. Cleared leaf samples were rinsed with 50% v/v
560 ethanol, then with water, and then stained in 150 mM K_2HPO_4 (pH 9.5) containing
561 0.01% w/v aniline blue for 30 min in the dark. Stained leaf samples were sectioned
562 and mounted in 50% v/v glycerol on slides. The slides were examined under a Zeiss
563 observer Z1 immunofluorescence microscope (Carl Zeiss MicroImaging GmbH,
564 Gottingen, Germany), and fluorescence intensity was determined using ImageJ
565 software.

566 Callose concentrations were measured using a plant callose ELISA kit (Catalog
567 number: JL46407; Jonln, Shanghai, China), according to the manufacturer's protocol.
568 The callose solution was prepared as follows: leaf material from the feeding site was
569 homogenized with PBS buffer (pH 7.4) and the mixture was centrifuged at 500–1000
570 g for 20 min. The supernatant was collected for the detection of callose concentration.
571 The absorbance at 450 nm was measured and callose concentrations were calculated
572 based on the standard curve.

573 ***RNA interference***

574 We conducted RNAi analyses to determine the function of LssaCA in mediating
575 RSV infection and regulating callose deposition. The *LssaCA*-specific gene fragment
576 was PCR-amplified with the primer pair LssaCA-T7F/LssaCA-T7R (Table S1). Then,
577 dsRNA was synthesized using a commercial kit (T7 RiboMAX Express RNAi System,
578 Promega, Madison, WI, USA) and purified by phenol: chloroform extraction and
579 isopropanol precipitation. Finally, 36.8 nL dsRNA at 1 ng/nL was delivered into the
580 insect hemocoel for gene silencing. Microinjection was performed using a glass
581 needle through a Nanoliter 2000 (World Precision Instruments, Sarasota, FL, USA).
582 The negative control, GFP dsRNA, was synthesized and microinjected following the
583 same protocol.

584 ***RT-qPCR***

585 Gene transcript levels were determined by RT-qPCR. The RNA was extracted
586 from *L. striatellus* tissues using an RNeasy Mini Kit (Qiagen, Hilden, Germany), and
587 from plant leaves using TRIzol. Reverse transcriptional PCR (iScript cDNA Synthesis
588 Kit, Bio-Rad, Hercules, CA, USA) and SYBR-Green-based qPCR (SYBR Green
589 Supermix, Bio-Rad) was performed according to the manufacturer's protocols. The
590 primer pair used to amplify *LssaCA* was LssaCA-q-F/LssaCA-q-R (Table S1). Viral
591 RNA copies were measured using the primers NP-q-F/NP-q-R (Table S1). *L.*
592 *striatellus* translation elongation factor 2 (*EF2*) and rice *actin* were amplified as
593 internal controls to ensure equal loading of cDNA isolated from different samples.
594 The primer pairs EF2-q-F/EF2-q-R and actin-q-F/actin-q-R (Table S1) were used to
595 amplify *EF2* and *actin*, respectively. Water was used as a negative control.

596 ***Yeast two-hybrid assays***

597 Yeast two-hybrid screening was performed to identify rice proteins interacting
598 with LssaCA. A high-complexity rice cDNA library was fused to *Gal4 AD* and
599 transformed into the yeast strain Y187. The *LssaCA* gene lacking the signal-peptide
600 sequence ($LssaCA^{sp-}$) was fused to *Gal4 DNA-BD* and transformed into the yeast
601 strain Y2HGold. The two yeast strains were co-cultured overnight to allow mating to

602 create diploids. After library screening, positive clones were selected on quadruple
603 dropout medium: SD/–Ade/–His/–Leu/–Trp supplemented with X-a-Gal and
604 aureobasidin A (QDO/X/A), and prey plasmids were isolated for sequencing. To
605 further confirm the interaction between LssaCA and OsTLP, *LssaCA*$^{sp-}$ was cloned
606 into the prey vector pDB-Leu, and the *OsTLP* gene lacking the signal-peptide
607 sequence (OsTLP^{sp-}) was cloned into the bait vector pPC86. The two plasmids were
608 co-transformed into the yeast stain Mav203 and the transformants were selected on
609 SD/–His–Leu–Trp + 20 mM 3-AT medium.
610
611 ***Pull-down assays***
612 Pull-down assays were performed to determine the molecular interactions
613 between LssaCA and RSV NP, LssaCA muteins and RSV NP, LssaCA and OsTLP,
614 and OsTLP and the LssaCA-NP complex.
615 The interaction between LssaCA and RSV NP was determined using GST
616 pull-down analyses as described previously (Huo et al., 2014). Briefly, *LssaCA*$^{sp-}$ was
617 cloned into the pGEX-3x vector and LssaCA was expressed as a GST-fusion protein
618 (GST-LssaCA). The *NP* gene was cloned into the pET-30a (+) expression vector and
619 the protein was expressed with an N-terminal His-tag (NP-His). The GST-LssaCA
620 construct was expressed in, and purified from, *E. coli* stain BL21. The GST-LssaCA
621 protein or the GST control protein was bound to Glutathione Sepharose beads (Cytiva,
622 Marlborough, MA, USA), then NP-His protein was added to the beads. The
623 bead-bound proteins were separated by SDS-PAGE and detected by western blotting
624 with antibodies against GST or His-tag.
625 We conducted His pull-down assays to determine the interactions between the
626 LssaCA muteins and RSV NP. The gene sequences encoding *LssaCA* muteins
627 (without the signal-peptide sequence) were each cloned into the pET-30a (+)
628 expression vector, and each mutein was expressed with an N-terminal His-tag. The
629 *NP* gene was cloned into the pGEX-3x vector and NP was expressed as a GST-fusion
630 protein (GST-NP). Each of the His-tag-fused LssaCA muteins was bound to Ni

631 Sepharose (GE Healthcare, Uppsala, Sweden), then the GST-NP protein or the GST
632 control protein was added to the beads. The bead-bound proteins were separated by
633 SDS-PAGE and detected by western blotting with antibodies against GST or His-tag.
634 Next, MBP pull-down analyses were performed to determine the interaction
635 between OsTLP and LssaCA. The *OsTLP*$^{sp-}$ sequence was cloned into pMAL-p2X to
636 produce the MBP-fusion protein (MBP-OsTLP). The MBP-OsTLP protein or the
637 MBP control protein was bound to amylose resin (New England Biolabs, Beverley,
638 MA, USA), and then the LssaCA-His protein was added to the beads. To determine
639 the interaction between OsTLP and the LssaCA-NP complex, the LssaCA-His and
640 GST-NP proteins were preincubated before being added to the beads. The bead-bound
641 proteins were separated by SDS-PAGE and detected by western blotting with the
642 MBP antibody (Cell Signaling Technology, Danvers, MA, USA), His-tag antibody
643 (Tiangen, Beijing, China) and GST antibody (Tiangen).

644 ***Microscale thermophoresis (MST) assays***

645 We conducted MST assays to detect the interactions between LssaCA and NP,
646 and between LssaCA and OsTLP. First, 10 μM purified LssaCA^{sp-} protein (His-fusion
647 protein) was labelled with a Monolith NT Protein Labeling Kit RED-NHS (Nano
648 Temper Technologies GMBH, München, Germany) using red fluorescent dye NT-647
649 N-hydroxysuccinimide (amine-reactive), according to the manufacturer's instructions.
650 The binding assays were performed on a Monolith NT.115 Microscale
651 Thermophoresis instrument (Nano Temper Technologies GMBH) using capillaries
652 treated using the standard method. The labeled protein LssaCA^{sp-} was added to
653 serially diluted NP (GST-NP, GST was used as a negative control) or OsTLP^{sp-}
654 (MBP-fusion protein, MBP was used as a negative control). The initial concentration
655 of each protein was 40 μM with 0.1% (v/v) Tween 20. The KD Fit function of
656 NanoTemper Analysis software version 1.2.214.1 was used for curve fitting and to
657 calculate the dissociation constant (Kd).

658 ***RSV inoculation through midrib microinjection***

659 Midrib microinjection was performed as described previously (Zhao et al., 2017).
660 Briefly, 200 RSV-infected *L. striatellus* were homogenized with 200 μL PBS (pH 7.0),
661 and the homogenate was centrifuged twice at 8000 g for 10 min at 4°C. The crude
662 virus extract was transferred to a new centrifuge tube. The concentration of RSV in
663 the extract was measured using a Nanodrop One instrument. The RSV extract was
664 adjusted to 1 mg/mL for microinjection. Rice seedlings were grown in an incubator
665 for 2 weeks until the leaf veins became clearly visible. Then, 23 nL RSV extract was
666 microinjected into the midrib. The RSV titers in plants were detected at 7–14 days
667 post microinjection.

668 ***β-1,3-glucanase activity***

669 β-1,3-glucanase hydrolyzes laminarin and cuts the β-1,3-glucoside bond to
670 produce a reducing terminus. Therefore, the rate of reducing sugars production was
671 used to calculate enzyme activity. One unit of β-1,3-glucanase activity was defined as
672 the amount of enzyme that hydrolyses laminarin to generate 1 μg reducing sugars per
673 minute.

674 The β-1,3-glucanase activity of OsTLP was measured using a beta-1,3-glucanase
675 microplate assay kit (Cat. ASK1028, Bioworld, Bloomington, MN, USA) according
676 to the manufacturer's instructions.

677 To determine the enzymatic activity of the recombinant OsTLP proteins, the
678 MBP-fusion OsTLP^{sp-} protein or the MBP control protein was adjusted to 0.5 mg/mL.
679 To determine the enzymatic activity of the *in vivo*-expressed OsTLP^{sp-}, 0.1 g rice leaf
680 material was homogenized with 1 mL assay buffer on ice, and then the mixture was
681 centrifuged at 12,000g at 4°C for 10 min. The supernatant was transferred into a new
682 centrifuge tube and kept on ice until detection of enzymatic activity.

683 For the assay, a 50-μL aliquot of the protein solution was mixed with laminarin
684 substrate and incubated at 37°C for 30 min. The reaction was terminated by
685 incubating the reaction tube in a boiling water bath for 10 min. The reaction
686 supernatant was transferred into a microplate and incubated at 90°C for 10 min before

measuring the absorbance at 540 nm.

Generation of transgenic plants

The full-length *OsTLP* gene was PCR-amplified with the primer pair TLP-F/TLP-R (Table S1), and cloned into the plant expression vector pCAMBIA-1300-eGFP to produce the plasmid pCAMBIA-1300-OsTLP. The plasmid pCAMBIA-1300-OsTLP was transformed into seedlings of the *Japonica* rice cultivar Nipponbare through *Agrobacterium*-mediated transformation as described previously (Hiei et al., 1994). Thirty independent T_0 transformants were obtained and were screened by germinating seeds from T_2 lines on medium containing 50 μg/ml hygromycin. The hygromycin-resistant homozygous seeds were used for further experiments. Seeds from homozygous lines transformed with the empty vector pCAMBIA-1300-eGFP were used as the negative control.

Statistical analyses

Graphs were constructed and statistical analyses were performed using Prism 9.0 software (GraphPad Software, San Diego, CA, USA). Data are expressed as the mean ± standard deviation (SD) calculated from three independent experiments. The significance of differences between two groups was determined by unpaired Student's t-test. Differences among three or more groups were compared using one-way analysis of variance (ANOVA).

Acknowledgments

This work is supported by the National Key R&D Program of China (2022YFD1400800), Major Program of the National Natural Science Foundation of China (32090013) and Youth Innovation Promotion Association CAS (2021084).

Author contributions

Conceptualization, Z.L.L., H.Y., Z.J.; Methodology, H.Y., Z.J. and Y.J.; Investigation, Z.J., Y.J., M.X.Y., H.Y.; Writing-Original Draft, H.Y. and Z.J.; Writing-Review & Editing, Z.L.L. and F.R.X.; Funding Acquisition, Z.L.L., H.Y. and F.R.X.; Supervision, Z.L.L., and F.R.X.

Declarations of competing interests

The authors declare no competing interests.

References

Acevedo, F.E., Smith, P., Peiffer, M., Helms, A., Tooker, J., and Felton, G.W. (2019). Phytohormones in fall armyworm saliva modulate defense responses in plants. J. Chem. Ecol. 45, 598-609. 10.1007/s10886-019-01079-z.

Arca, B., and Ribeiro, J.M. (2018). Saliva of hematophagous insects: a multifaceted toolkit. Curr. Opin. Insect Sci. 29, 102-109. 10.1016/j.cois.2018.07.012.

Bonaventure, G. (2012). Perception of insect feeding by plants. Plant Biol. (Stuttg.) 14, 872-880. 10.1111/j.1438-8677.2012.00650.x.

Bucher, G.L., Tarina, C., Heinlein, M., Serio, F.D., Jr, F.M., and Iglesias, V.A. (2001). Local expression of enzymatically active class I β-1, 3-glucanase enhances symptoms of TMV infection in tobacco. Plant J. 28, 361-369. 10.1046/j.1365-313x.2001.01181.x.

Conway, M.J., Londono-Renteria, B., Troupin, A., Watson, A.M., Klimstra, W.B., Fikrig, E., and Colpitts, T.M. (2016). *Aedes aegypti* D7 saliva protein inhibits *Dengue virus* infection. PLoS Negl. Trop. Dis. 10, e0004941. 10.1371/journal.pntd.0004941.

de Jesus-Pires, C., Ferreira-Neto, J.R.C., Pacifico Bezerra-Neto, J., Kido, E.A., de Oliveira Silva, R.L., Pandolfi, V., Wanderley-Nogueira, A.C., Binneck, E., da Costa, A.F., Pio-Ribeiro, G., et al. (2020). Plant thaumatin-like proteins: function, evolution and biotechnological applications. Curr. Protein Pept. Sci. 21, 36-51.

10.2174/1389203720666190318164905.

Hao, P.Y., Liu, C.X., Wang, Y.Y., Chen, R.Z., Tang, M., Du, B., Zhu, L.L., and He, G.C. (2008). Herbivore-induced callose deposition on the sieve plates of rice: an important mechanism for host resistance. Plant Physiol. 146, 1810-1820. 10.1104/pp.107.111484.

Hermance, M.E., and Thangamani, S. (2015). Tick saliva enhances *Powassan virus* transmission to the host, influencing its dissemination and the course of disease. J. Virol. 89, 7852-7860. 10.1128/JVI.01056-15.

Hiei, Y., Ohta, S., Komari, T., and Kumashiro, T. (1994). Efficient transformation of rice (*Oryza sativa L.*) mediated by *Agrobacterium* and sequence analysis of the boundaries of the T-DNA. Plant J. 6, 271-282. 10.1046/j.1365-313x.1994.6020271.x.

Hipper, C., Brault, V., Ziegler-Graff, V., and Revers, F. (2013). Viral and cellular factors involved in Phloem transport of plant viruses. Front. Plant Sci. 4, 154. 10.3389/fpls.2013.00154.

Huang, H.J., Liu, C.W., Xu, H.J., Bao, Y.Y., and Zhang, C.X. (2017). Mucin-like protein, a saliva component involved in brown planthopper virulence and host adaptation. J. Insect Physiol. 98, 223-230. 10.1016/j.jinsphys.2017.01.012.

Huo, Y., Zhao, J., Meng, X.Y., Yang, J., Zhang, Z.Y., Liu, Z.W., Fang, R.X., and Zhang, L.L. (2022). *Laodelphax striatellus* saliva mucin enables the formation of stylet sheathes to facilitate its feeding and *rice stripe virus* transmission. Pest Manag. Sci. 78(8), 3498-3507. 10.1002/ps.6990.

Ji, R., Ye, W.F., Chen, H.D., Zeng, J.M., Li, H., Yu, H.X., Li, J.C., and Lou, Y.G. (2017). A salivary endo-beta-1,4-glucanase acts as an effector that enables the Brown Planthopper to feed on rice. Plant Physiol. 173, 1920-1932. 10.1104/pp.16.01493.

Lou, Y.H., Shen, Y., Li, D.T., Huang, H.J., Lu, J.B., and Zhang, C.X. (2019). A mucin-like protein is essential for oviposition in *Nilaparvata lugens*. Front. Physiol. 10, 551. 10.3389/fphys.2019.00551.

Ramamoorthi, N., Narasimhan, S., Pal, U., Bao, F., Yang, X.F., Fish, D., Anguita, J., Norgard, M.V., Kantor, F.S., Anderson, J.F., et al. (2005). The Lyme disease agent

769 exploits a tick protein to infect the mammalian host. Nature 436, 573-577.
770 10.1038/nature03812.
771 Schuijt, T.J., Hovius, J.W., van Burgel, N.D., Ramamoorthi, N., Fikrig, E., and
772 van Dam, A.P. (2008). The tick salivary protein Salp15 inhibits the killing of
773 serum-sensitive *Borrelia burgdorferi* sensu lato isolates. Infect. Immun. 76,
774 2888-2894. 10.1128/IAI.00232-08.
775 Shangguan, X.X, Zhang, J., Liu, B.F., Zhao, Y., Wang, H.Y., Wang, Z.Z., Guo,
776 J.P., Rao, W.W., Jing, S.L., Guan, W., et al. (2018). A mucin-Like protein of
777 planthopper is required for feeding and induces immunity response in plants. Plant
778 Physiol. 176, 552-565. 10.1104/pp.17.00755.
779 Sun, P., Nie, K.X., Zhu, Y.B., Liu, Y., Wu, P., Liu, Z.W., Du, S.Y., Fan, H.H.,
780 Chen, C.H., Zhang, R.L., et al. (2020). A mosquito salivary protein promotes
781 flavivirus transmission by activation of autophagy. Nat. Commun. 11, 260.
782 10.1038/s41467-019-14115-z.
783 Tjallingii, W.F. (2006). Salivary secretions by aphids interacting with proteins of
784 phloem wound responses. J. Exp. Bot. 57, 739-745. 10.1093/jxb/erj088.
785 van Bel, A.J., and Will, T. (2016). Functional evaluation of proteins in watery
786 and gel saliva of aphids. Front. Plant Sci. 7, 1840. 10.3389/fpls.2016.01840.
787 Verpoorte, J.A., Mehta, S., and Edsall, J.T. (1967). Esterase activities of human
788 carbonic anhydrases B and C. J. Biol. Chem. 242, 4221-4229.
789 10.1016/s0021-9258(18)95800-x.
790 Wang, X.W., and Blanc, S. (2021). Insect transmission of plant single-stranded
791 DNA viruses. Annu. Rev. Entomol. 66, 389-405.
792 10.1146/annurev-ento-060920-094531.
793 Wen, S.Y., Wang, F., Ji, Z.H., Pan, Y.Y., Jian, M.M, Bi, Y.F., Zhou, G.Z., Luo,
794 L.S., Chen, T.G., Li, L.B., et al. (2019). Salp15, a multifunctional protein from tick
795 saliva with potential pharmaceutical effects. Front. Immunol. 10, 3067.
796 10.3389/fimmu.2019.03067.
797 Will, T., and Vilcinskas, A. (2015). The structural sheath protein of aphids is

required for phloem feeding. Insect. Biochem. Mol. Biol. 57, 34-40. 10.1016/j.ibmb.2014.12.005.

Wu, W., Zheng, L., Chen, H., Jia, D., Li, F., and Wei, T. (2014). Nonstructural protein NS4 of *rice stripe virus* plays a critical role in viral spread in the body of vector insects. PLoS One 9(2), e88636. 10.1371/journal.pone.0088636.

Wu, W., Yi, G., Lv, X.W., Mao, Q.Z., and Wei, T.Y. (2022). A leafhopper saliva protein mediates horizontal transmission of viral pathogens from insect vectors into rice phloem. Commun. Biol. 5, 204. 10.1038/s42003-022-03160-y.

Xu, Y., Fu, S., Tao, X.R, and Zhou, X. P. (2021). *Rice stripe virus*: exploring molecular weapons in the arsenal of a negative-sense RNA virus. Annu. Rev. Phytopathol. 59, 351-371. 10.1146/annurev-phyto-020620-113020.

Yi, G., Wu, W., and Wei, T.Y. (2021). Delivery of *rice gall dwarf virus* into plant phloem by its leafhopper vectors activates callose deposition to enhance viral transmission. Front. Microbiol. 12, 662577. 10.3389/fmicb.2021.662577.

Zavaliev, R., Ueki, S., Epel, B.L., and Citovsky, V. (2011). Biology of callose (beta-1,3-glucan) turnover at plasmodesmata. Protoplasma 248, 117-130. 10.1007/s00709-010-0247-0.

Zhao, W., Kang, L., and Cui, F. (2017). Isolation of *rice stripe virus* preparation from viruliferous Small Brown Planthoppers and mechanic inoculation on rice. Bio. Protoc. 7, e2597. 10.21769/BioProtoc.2597.

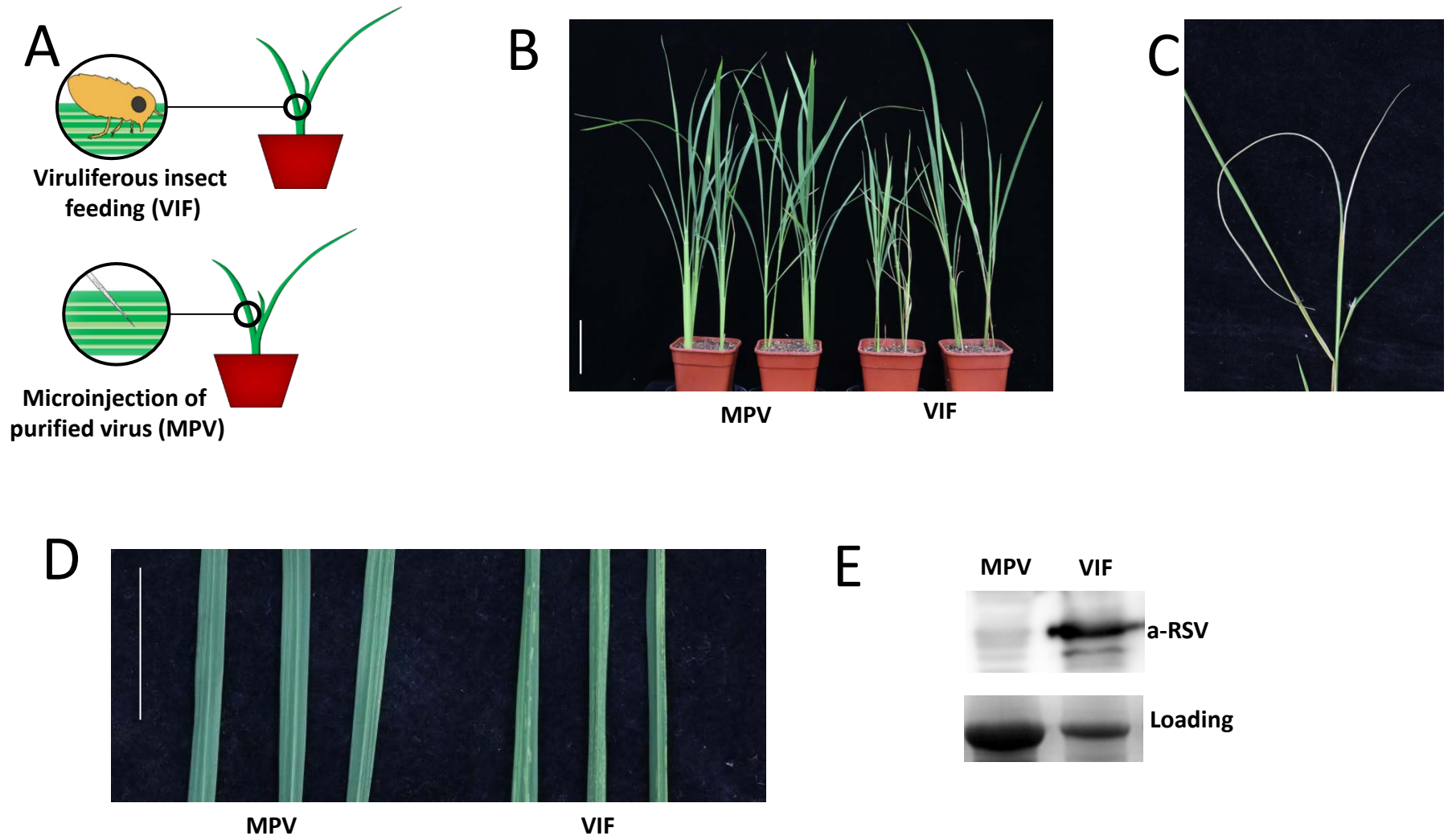

Figure 1. *Laodelphax striatellus* feeding is necessary for *Rice stripe virus* (RSV) to infect rice.
A. The schematic diagram shows the two methods of rice inoculation with RSV: viruliferous insect feeding (VIF) and microinjection of purified virus (MPV). Three-leaf rice seedlings were used and viral infection was detected three weeks after inoculation.
B-D. Plant symptoms of rice stripe disease were observed in the VIF group (B-D), including heart leaf curling (C) and the striped spots on the leaves (D), but not in the MPV group (B and D). C shows an enlarged image of the VIF-group leaves.
E. Western blots to show the levels of RSV infection in plants inoculated with VIF or MPV. Anti-RSV antibodies were used to detect the RSV titers in the plants.

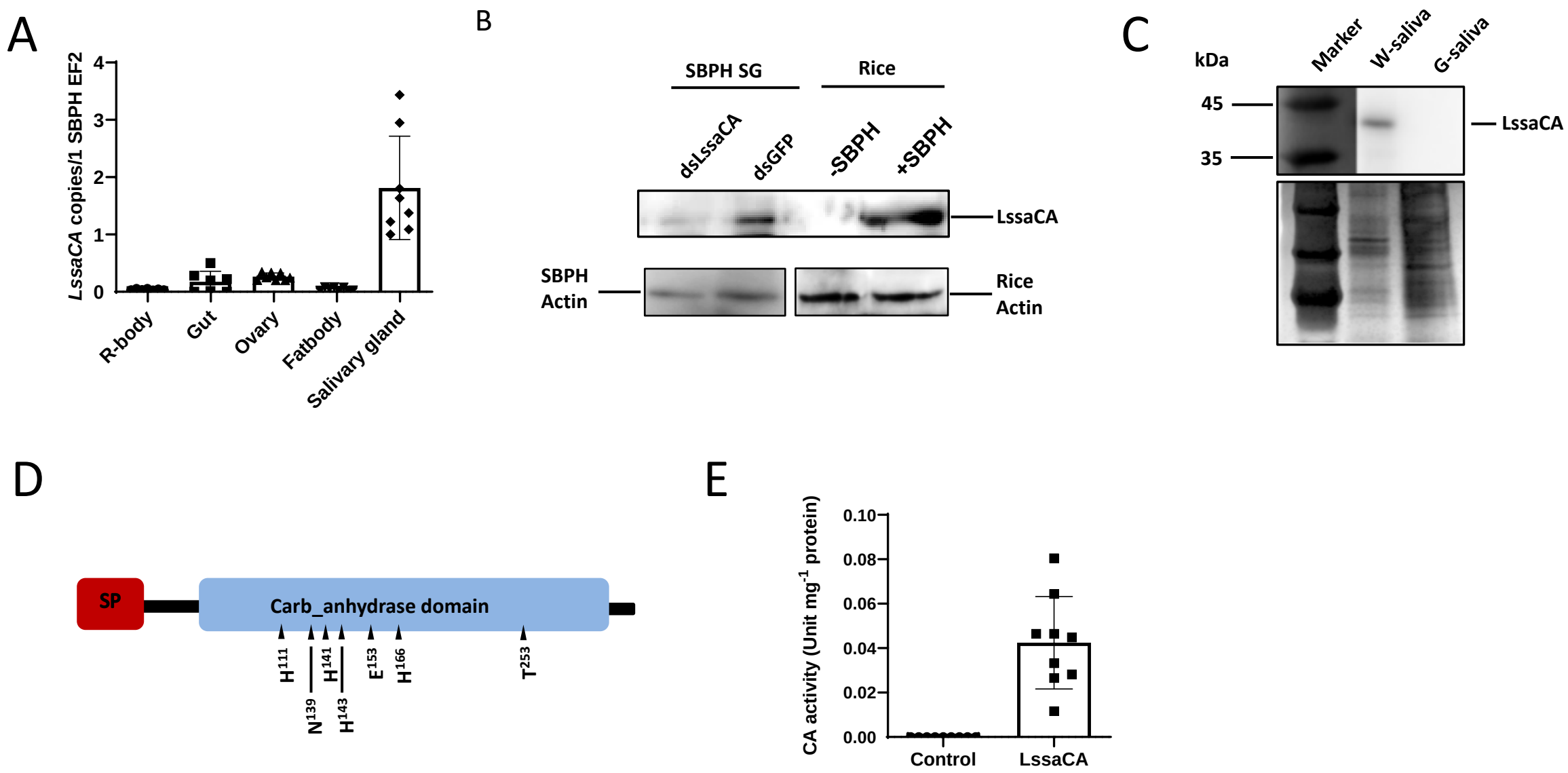

Figure 2. Characteristics of the *L. striatellus* saliva carbonic anhydrase (LssaCA).

A. RT-qPCR analyses of *LssaCA* transcript levels in different tissues. R-body, the remaining body after removal of the guts, salivary glands, fat bodies, and ovaries.

B. Western blots showing LssaCA protein distribution in *L. striatellus* salivary glands (SBPH SG) and rice plants (Rice). The weaker signal in dsLssaCA-treated SBPH indicates a specific knockdown of LssaCA by dsLssaCA. Rice plants fed by SBPH acquire LssaCA (+SBPH), whereas control plants do not contain LssaCA protein (-SBPH).

C. Western blots showing the distribution of LssaCA in watery and gel saliva. Total watery or gel saliva proteins were detected by silver staining.

D. Schematic diagram of LssaCA protein sequence. SP, signal peptide; Carb_anhydrase domain, conserved eukaryotic-type carbonic anhydrase sequence. Triangles indicate seven predicted catalytically active residues.

E. Esterase activity of recombinantly expressed LssaCA protein.

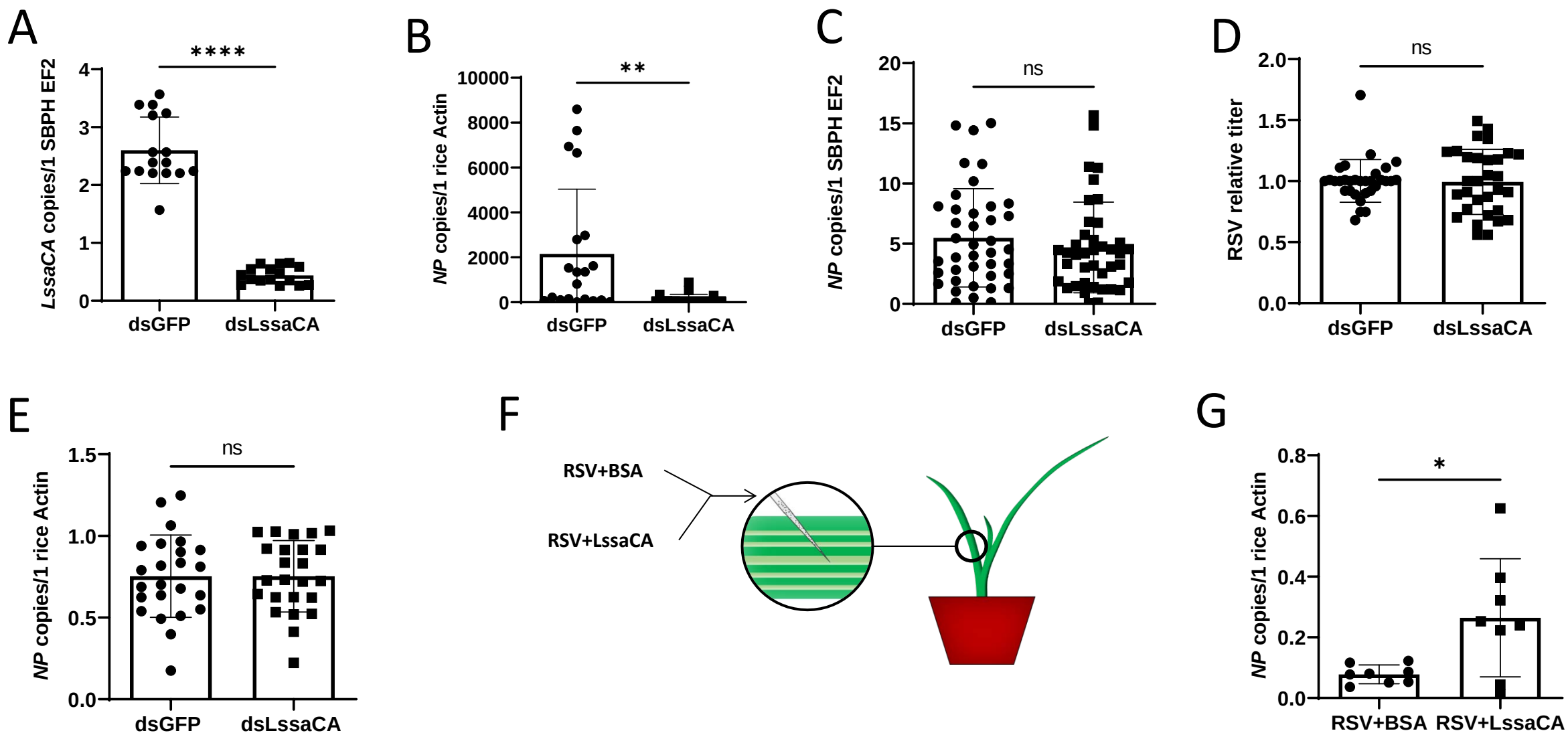

Figure 3. The influence of LssaCA deficiency on RSV transmission and viral infection of plants.

A. The efficiency of gene silencing as determined by RT-qPCR. Each dot represents salivary glands from five RSV-infected third-instar nymphs.

B. RSV infection level in rice plants as determined by RT-qPCR. RSV infection levels are represented by the copy number of the NP gene. Each dot represents one rice plant fed on for 2 d and then grown for another 14 d.

C. RSV titers in L. striatellus salivary glands as determined by RT-qPCR. Each dot represents salivary glands from five RSV-infected third-instar nymphs.

D. RSV titers in L. striatellus saliva as determined by RT-qPCR. Each dot represents one saliva sample from 10 insects fed with an artificial diet.

E. RSV titers in rice plants as determined by RT-qPCR. Rice plants were fed for 24 h and RSV titers were assayed immediately post-feeding. Each dot represents one rice plant.

E.Schematic diagram to show the process of microinjecting an RSV particle solution into a plant. The RSV was pre-incubated with BSA or recombinantly expressed LssaCA protein before being microinjected into the plant phloem.

F. RT-qPCR to determine the level of RSV infection in microinjection-inoculated rice. The titers of RSV (copy number of NP) in rice plants were measured at 14 days post-inoculation (dpi). BSA was used as a negative control. *, $p < 0.05$.

DsLssaCA and dsGFP indicate LssaCA- and GFP-specific dsRNA, respectively. ****, $p < 0.0001$; **, $p < 0.01$; ns, not significant.

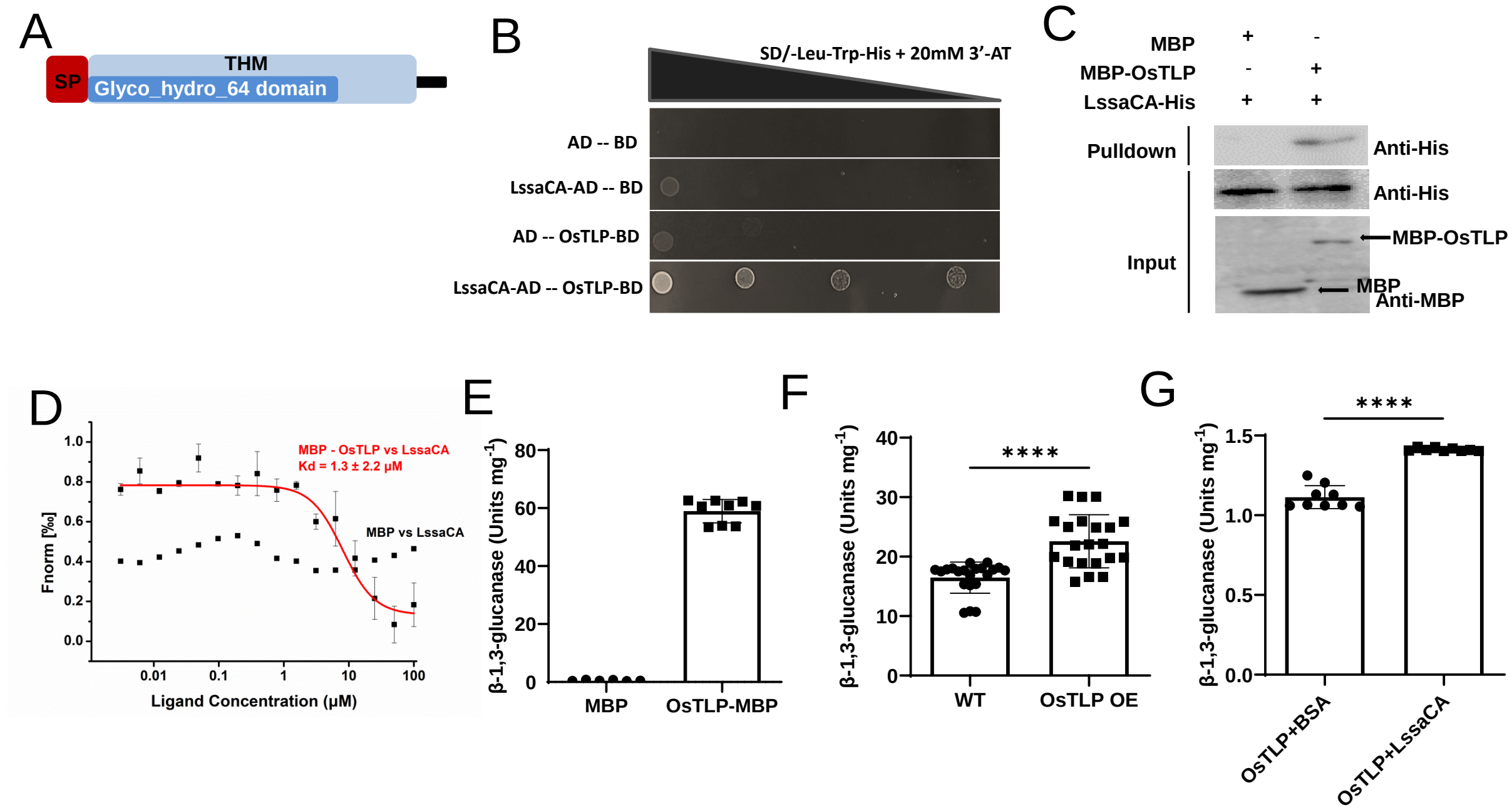

Figure 4. The interaction between OsTLP and LssaCA plays a role in regulating the enzymatic activity of OsTLP.

A. Schematic diagram of the OsTLP protein sequence. SP, signal peptide; THM, conserved thaumatin family protein sequence. Glyco_hydro_64 domain, glycoside hydrolases of family 64.

B. Yeast two-hybrid assay showing the interaction between OsTLP and LssaCA. SD, synthetically defined medium; Leu, Leucine; Trp, Tryptophan; His, Histidine; 3'AT, 3-amino-1,2,4-triazole; AD, transcription activation domain; BD, DNA-binding domain.

C.Pull-down assays showing the interactions between LssaCA (LssaCA-His) and OsTLP (MBP-OsTLP). MBP was used as a negative control. Both anti-His and anti-MBP antibodies were used to detect corresponding proteins.

D. MST assay showing the interaction between LssaCA (LssaCA-His) and OsTLP (MBP-OsTLP). MBP was used as a negative control. Bars represent SE.

E. The endo-β-1,3-glucanase activity of the purified recombinant OsTLP protein (expressed as MBP-fusion protein). MBP was used to normalize results.

F. The endo-β-1,3-glucanase activity of OsTLP, which was overexpressed in transgenic plants (OsTLP OE) or wild-type plants (WT).

G. Regulation of OsTLP enzymatic activity by LssaCA. ****, $p < 0.0001$.

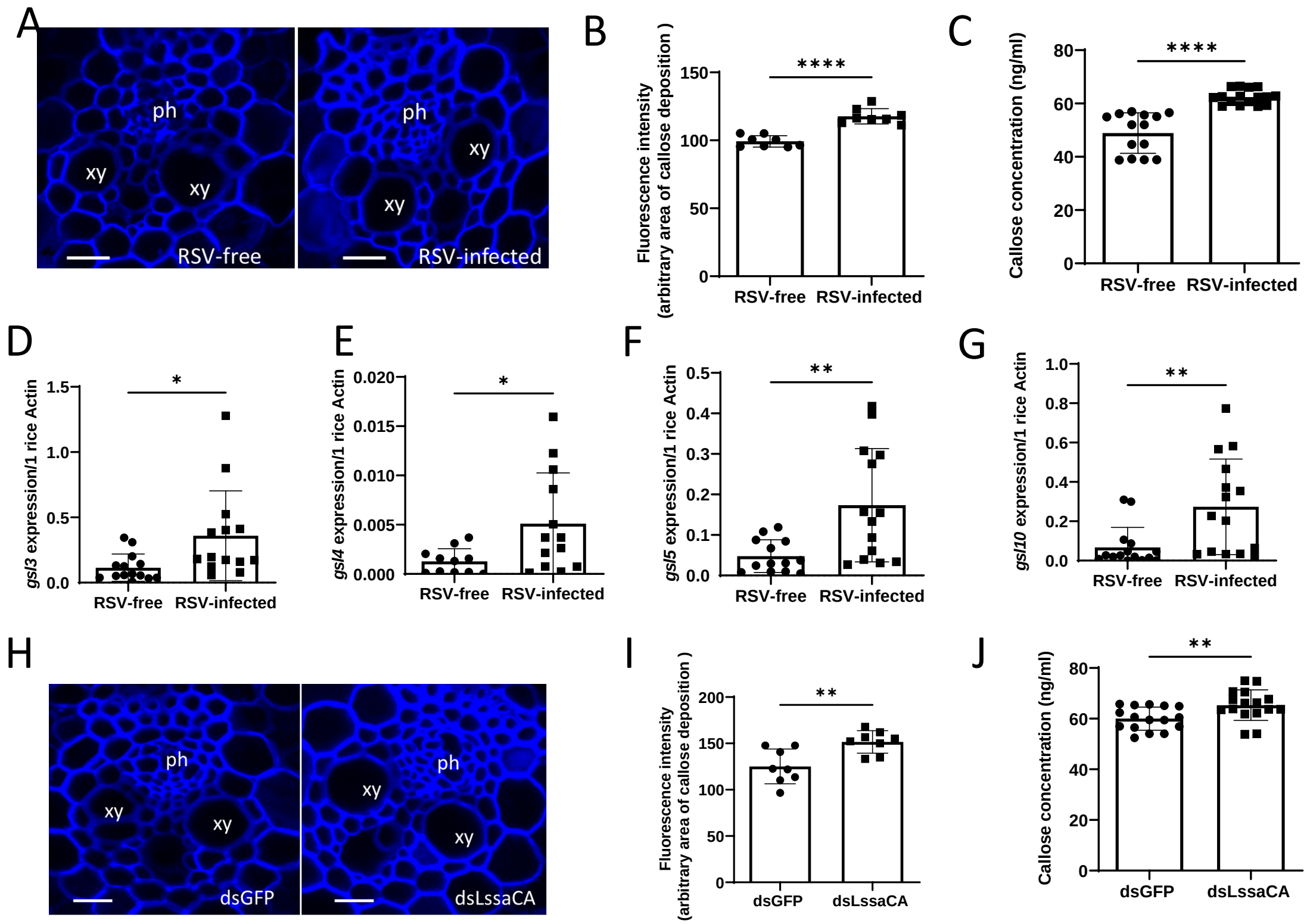

Figure 5. LssaCA inhibits RSV-induced callose deposition.

A. Bright blue fluorescence of cross-sections showing callose deposition at feeding sites. Samples were prepared from the leaf phloem of plants fed on by RSV-free or RSV-infected L. striatellus. Thin sections were stained with 0.1% aniline blue at 24 h after L. striatellus feeding and examined under a fluorescence microscope. Xy, xylem; ph, phloem. Scale bars: 20 μm.

B.Average fluorescence intensity of arbitrary area of callose deposition counted using ImageJ. Eight to ten random sites per sample were selected for the evaluation of fluorescence intensity. ****, $p < 0.0001$.

C.Callose concentration in leaves of rice plants fed on by RSV-free or RSV-infected L. striatellus. ****, $p < 0.0001$.

D–G. Transcript levels of callose synthase genes as determined by RT-qPCR. Insects were allowed to feed on rice plants for 24 h before total RNAs were extracted. *, $p < 0.05$; **, $p < 0.01$.

H. Bright blue fluorescence of cross-sections showing callose deposition at feeding sites. Samples were prepared from leaf phloem of plants fed on by dsGFP- or dsLssaCA-treated RSV-infected L. striatellus. Thin sections were stained with 0.1% aniline blue at 24 h after L. striatellus feeding and examined under a fluorescence microscope. Xy, xylem; ph, phloem. Scale bars: 20 μm.

I. Average fluorescence intensity of arbitrary area of callose deposition counted using ImageJ under a fluorescence microscope. Eight to ten random sites per sample were selected for the evaluation of fluorescence intensity. **, $p < 0.01$.

J. Callose concentration in leaves of rice plants fed on by dsGFP- or dsLssaCA-treated L. striatellus. **, $p < 0.01$.

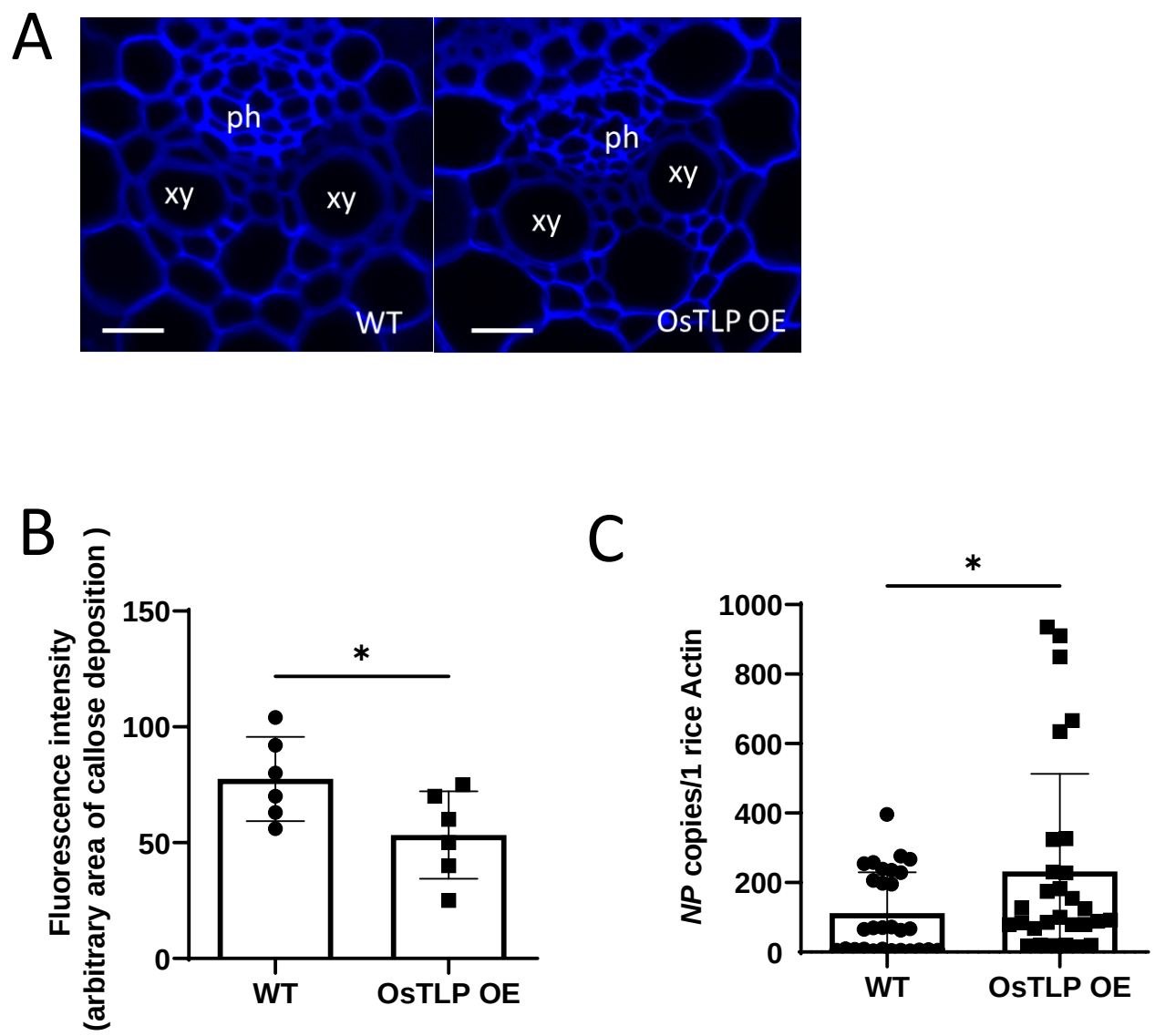

Figure 6. OsTLP inhibits callose deposition to facilitate RSV infection.

A. Bright blue fluorescence of cross-sections showing callose deposition at feeding sites. Samples were prepared from the leaf phloem of plants fed on by RSV-infected L. striatellus. Scale bars: 20 μm. OsTLP OE, transgenic plants over-expressing OsTLP.

B. Average fluorescence intensity of arbitrary area of callose deposition counted using ImageJ under a fluorescence microscope. *, $p < 0.05$.

C.Promotion of RSV infection by OsTLP overexpression, as determined by RT-qPCR. Titers of RSV (copy number of NP) were measured at 14 days post-feeding. *, $p < 0.05$.

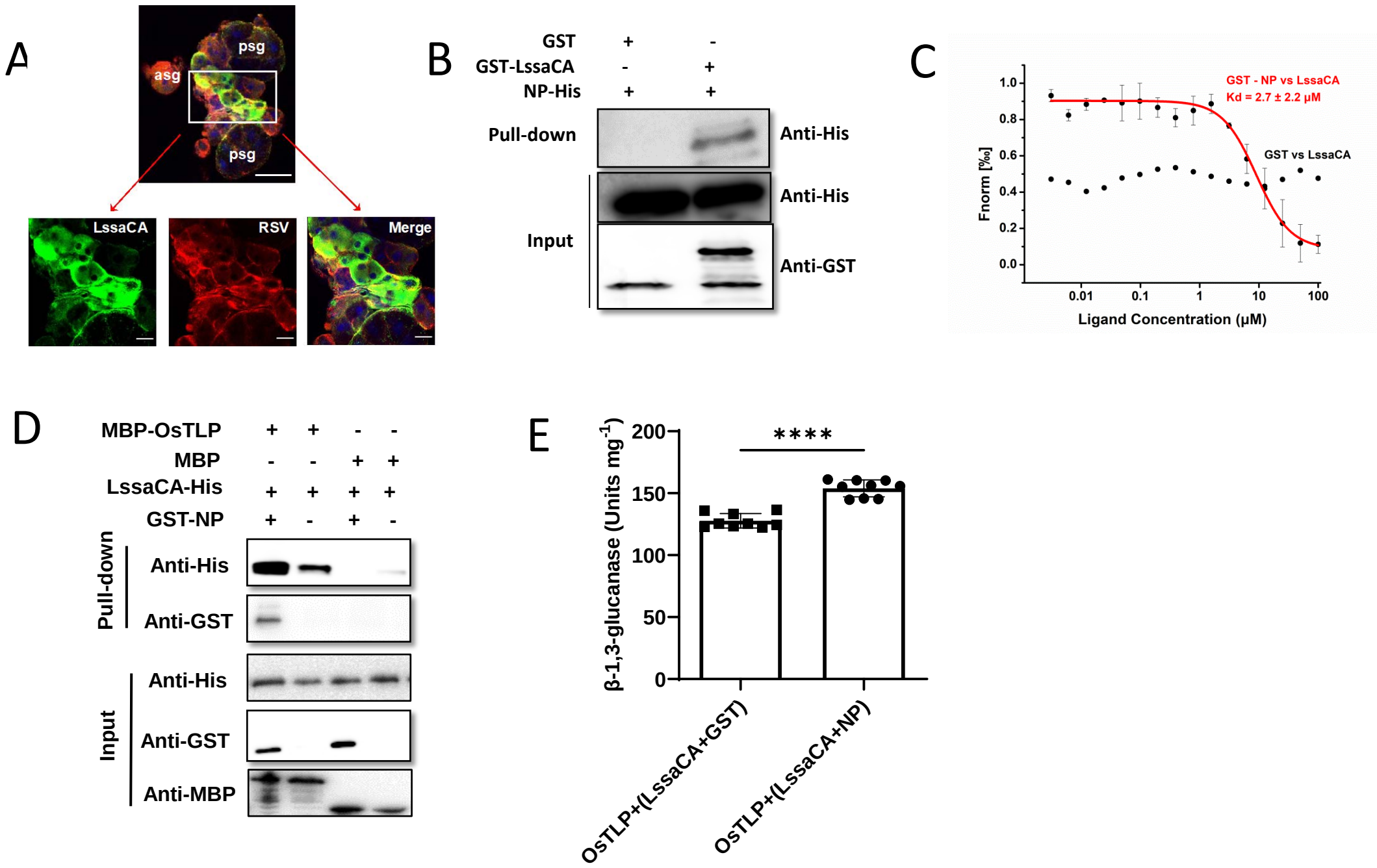

Figure 7. LssaCA-RSV NP interaction enhances the OsTLP enzymatic activity.
A.Immunofluorescence assay showing co-localization of RSV (shown in red) and LssaCA (shown in green) in L. striatellus salivary glands. Images are representative of three independent experiments with a total of 30 SBPHs analyzed. The scale bar represents 20 μm. psg, principal salivary gland; asg, accessory salivary gland.
B.GST pull-down assays show the interaction between LssaCA (GST-LssaCA) and RSV NP (NP-His). GST was used as a negative control. Anti-GST and anti-His antibodies were used to detect the corresponding proteins.
C.MST assay showing the interaction between LssaCA (LssaCA-His) and RSV NP (GST-NP). GST was used as a negative control. Bars represent SE.
D.Pull-down assays showing the interaction between OsTLP (MBP-OsTLP) and LssaCA-NP complex. LssaCA was expressed with a His tag and RSV NP was expressed as a GST-fusion protein. LssaCA and NP were preincubated before co-incubation with OsTLP. Anti-His and anti-GST antibodies were used to detect the corresponding proteins.
E.Regulation of OsTLP enzymatic activity by LssaCA and LssaCA-NP. (LssaCA + NP) indicates that the two proteins were pre-incubated before incubation with OsTLP. ****, $p < 0.0001$.

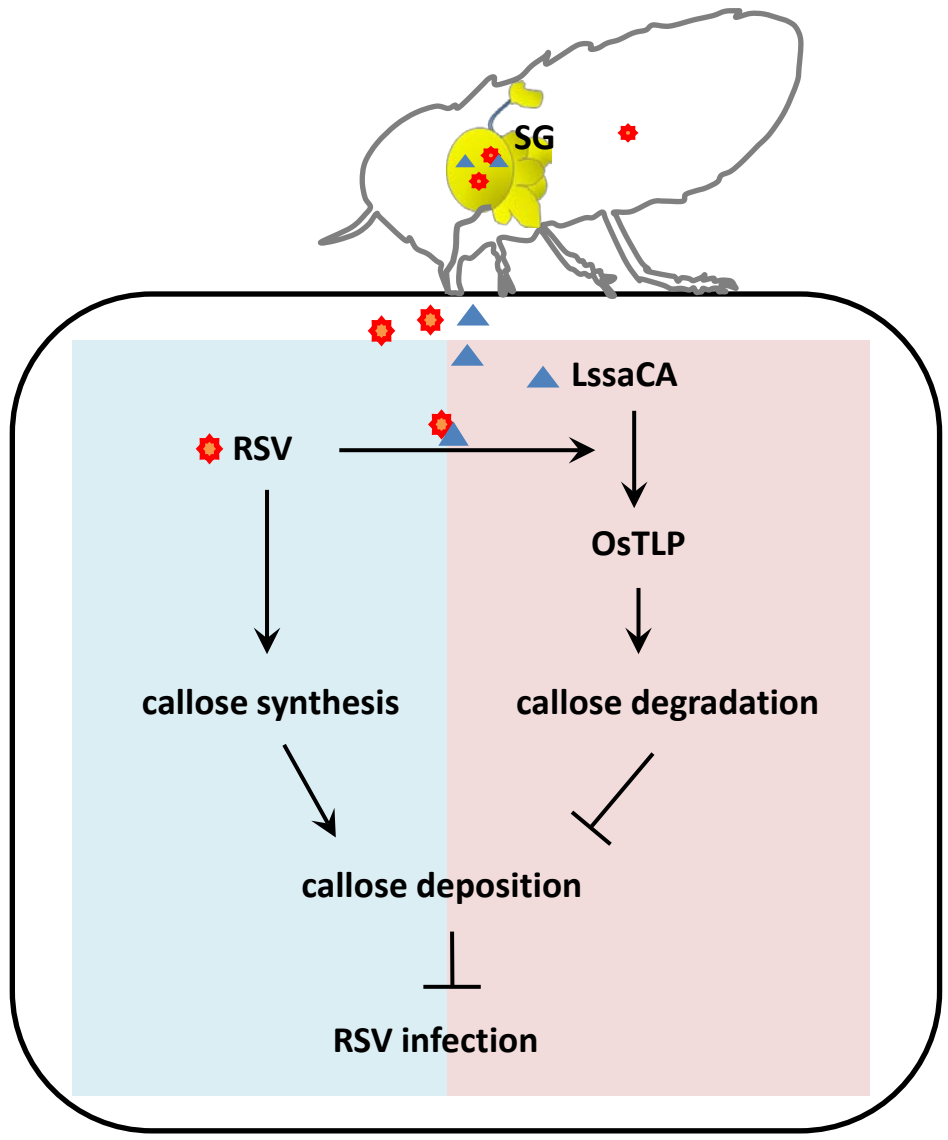

Figure 8. Proposed model of how RSV NP-LssaCA-OsTLP tripartite interaction leads to callose degradation to promote RSV infection of plants.

L. striatellus feeding on rice plants inoculates both RSV and LssaCA into the phloem sieve elements. Within the plants, RSV induces callose synthesis, causing callose deposition to inhibit RSV infection. However, LssaCA reverses this inhibition by binding to OsTLP to enhance its β-1,3-glucanase activity, which degrades the deposited callose. The interaction between RSV and LssaCA further enhances the OsTLP enzymatic activity and facilitates RSV infection.